



Curie temperature of Nanoparticle Sized Aluminium Substituted Copper Cobalt Ferrites

S.S. Karande¹, M.S. Kavale¹, B. R. Karche²

¹Department of Physics, Sangameshwar College, Solapur, Maharashtra, India

²Material Science and Thin Film Laboratory, Shankarrao Mohite Mahavidyalaya, Akulj, Dist: Solapur, Maharashtra, India

ABSTRACT

The polycrystalline aluminium substituted nano-particle sized copper cobalt ferrite samples $Cu_xCo_{1-x}Fe_{2-2y}Al_{2y}O_4$ (where $x = 0.0, 0.2, 0.4, 0.6, 0.8, 1.0$; $y = 0.05, 0.15$ and 0.25) have been prepared by standard ceramic technique. Phase formation is investigated using X-ray diffraction, Infrared absorption technique and Scanning electron microscope technique. The lattice constants of the all samples are evaluated from x-ray diffraction data. Curie temperature of samples goes on decreases with addition of aluminium and copper in the host lattice of cobalt ferrite.

Keywords : Polycrystalline, nanoparticle size, standard ceramic technique and Inverse cubic spinel, Curie temperature

I. INTRODUCTION

In a way, every material utilized today is a composite. Composite materials are a physical mixture of two or more compatible micro or macro constituent particles which differ in form and chemical composition and are essentially insoluble in each other. Composite materials are best suited for scientific applications which could not be achieved by any one component acting on its own. Ferrite / ferroelectric composites are termed as magneto electric (ME) composites due to the coupling between the electric and magnetic fields in the materials. The conversion of magnetic to electric fields in such ME composite originates from the elastic interaction between ferrite and ferroelectric subsystems [1]. In the presence of the magnetic field, the magnetostriction in the ferrite phase gives rise to mechanical stresses that are

transferred to the ferroelectric phase, resulting in electric polarization of the ferroelectric phase owing to its magneto electric effect. ME materials find applications as smart materials in actuators, sensors, magnetic probes, phase inverters, rectifiers, modulators, and transducers in solid state microelectronics and microwave devices [2,3]. Spinel ferrite nanoparticles are being intensively investigated in recent years because of their remarkable electrical and magnetic properties and wide practical applications in information storage system, ferro-fluid technology, magnetocaloric refrigeration and medical diagnosis [4]. Among the spinels, mixed Zn ferrites and especially Ni-Zn ferrites are widely used in applications like transformer cores, chokes, coils, noise filters recording heads etc. [5]. While Ni-Zn ferrite possesses higher resistivity and saturation magnetization, cobalt

ferrite possess high cubic magneto crystalline anisotropy and hence high coercivity. The high coercivity is driven by large anisotropy of the cobalt ions due to its important spin orbit coupling. It is ferromagnetic with a Curie temperature (T_c) around 520°C, [6] and shows a relatively large magnetic hysteresis which distinguishes it from rest of the spinels. The synthesis of ultra fine magnetic particles has been extensively investigated in recent years because of their potential applications in high density magnetic recording and magnetic fluids [7]. Among the current methods for synthesis of mixed ferrite the combustion reaction method stands out as an alternative and highly promising method for the synthesis of these ferrites [8]. Magnetic properties measured at room temperature by vibrating sample magnetometer (VSM) reveal an increase in saturation magnetization with increase in cobalt concentration [9].

II. EXPERIMENTAL

Materials:

High purity starting materials are used as Cobalt Oxide (CoO):- 74.9326 gm, Copper Oxide (CuO):- 74.5454 gm, Ferric oxide(Fe_2O_3):- 159.6922 gm, Aluminum Oxide (Al_2O_3):- 101.9612 gm

Preparation of ferrite:

Nano crystalline powder samples of $Cu_xCo_{1-x}Fe_{2-2y}Al_{2y}O_4$ (where $x= 0.0, 0.2, 0.4, 0.6, 0.8, 1.0$; $y = 0.05, 0.15$ and 0.25) were prepared by the standard ceramic technique. Starting materials CuO, CoO, Fe_2O_3 and Al_2O_3 of AR grade obtained from Sigma – Aldrich, India were used. These samples were heated at ramping rate of $80\text{ }^\circ\text{C hr}^{-1}$ at 1000°C for 48 hours. XRD and IR analysis revealed the cubic spinel structure of the synthesized samples and functional groups in the samples respectively. The absence of any extra line confirms the formation of single phase ferrite. The average particle size 'D' was determined from line broadening (311) reflection using the Debye

Scherer formula discussed elsewhere [10]. Calculations of lattice constant, physical density, X-ray density, porosity, site radii and ionic bond lengths on both sites were calculated by using formulae discussed elsewhere [11] and graphically shown in fig.4. Infrared absorption spectra of powdered samples were recorded in the range $350\text{-}800\text{ cm}^{-1}$ using Perkin-Elmer FTIR spectrum and spectrometer by KBr pellet technique and presented in (fig.2). The scanning electron microscopes are shown in fig.3

III. RESULTS AND DISCUSSION

The X-ray diffraction patterns of the samples are presented in (fig.1). Powder X-ray diffractometer of the ferrite samples reveals the single phase spinel structure, as well defined reflection is observed without any ambiguity. The diffraction peaks are corresponding to (200), (311), (400), (422), (333/511), (440) and (533) planes. The lattice constants 'a' and 'c' for all prepared samples are calculated by using prominent (311) XRD peak. The calculated and observed values of inter planer distance (d) are found in good agreement with each other for all reflections. The physical density (dB), x-ray density (dx), and porosity (p), are calculated from the formulae given by Gadkari et.al [12].

From the calculations of lattice constants 'a' and 'c' for all the prepared ferrites it is observed that $c > a$ and tetragonality ratio (c/a) is found in the range of 1.03 to 1.07. This result is in good agreement with previous report [13-14]. In this present report tetragonality ratio for copper ferrite is 1.06. It means 70% copper resides on B site and it exhibits prorate type distortions in the crystal lattice. The previous report [15] well supports the present results reported this communication. Both Fe^{3+} and Cu^{2+} are John-Teller ion which produces prorate type distortions on (B) site and hence $c > a$ and $(c/a) = 1.06$. Therefore copper ferrite exhibits tetragonal spinel structure in host crystal lattice of cobalt ferrite. In addition of copper content in tetragonality ratio is found

increasing but due to addition of aluminium tetragonality ratio decreases. It means that Al^{3+} and copper suppress the tetragonal prolate type.

The crystallite sizes (t) of all the prepared samples were computed by Scherer rule utilizing the peak width at one-half intensity of the maximum intensity peak (311).

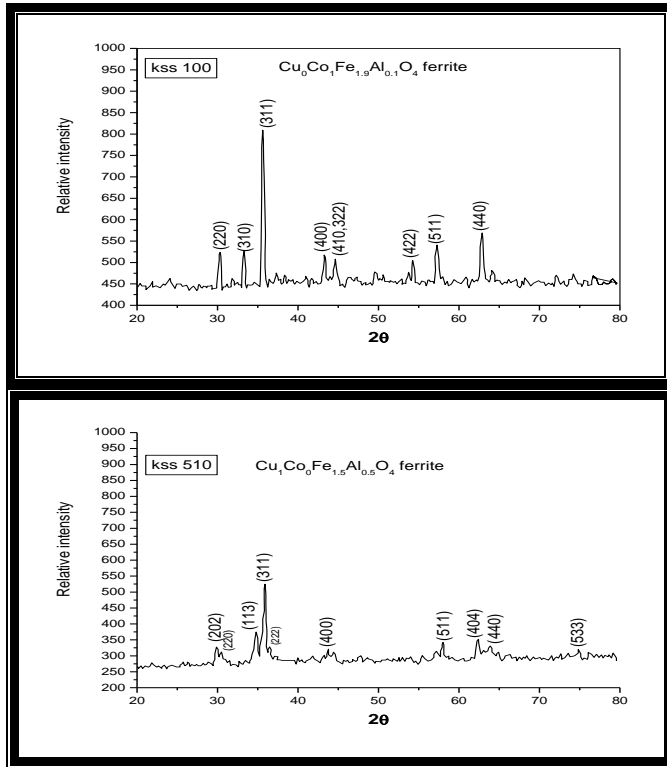


Fig: 1 XRD patterns of system $Cu_xCo_{1-x}Fe_{2-2y}Al_{2y}O_4$

The Al ($y = 0.05-0.25$) doped copper cobalt ferrite samples show a higher grain growth and the crystallite size (t) lies in the extent of 52.53-94.4 nm. The mean particle size calculated from diffractograms is in the range of 50 to 100 nm. That suggest the particles in the ferrites samples are fine and there is continuous grain growth in all compositions. It gives the confirmation of suitable microstructure formation in all compositions. The width of the reflection peak (311) for all the compositions is approximately the same due to the nearly equal particle size.

The infrared absorption spectra are showing two distinct absorption bands ν_1 due to tetrahedral (A) site interstitial voids near 600 cm^{-1} and other ν_2 due to octahedral (B) site interstitial voids near 400 cm^{-1} .

Our results in this present communication are well supported by previous reports [16, 17].

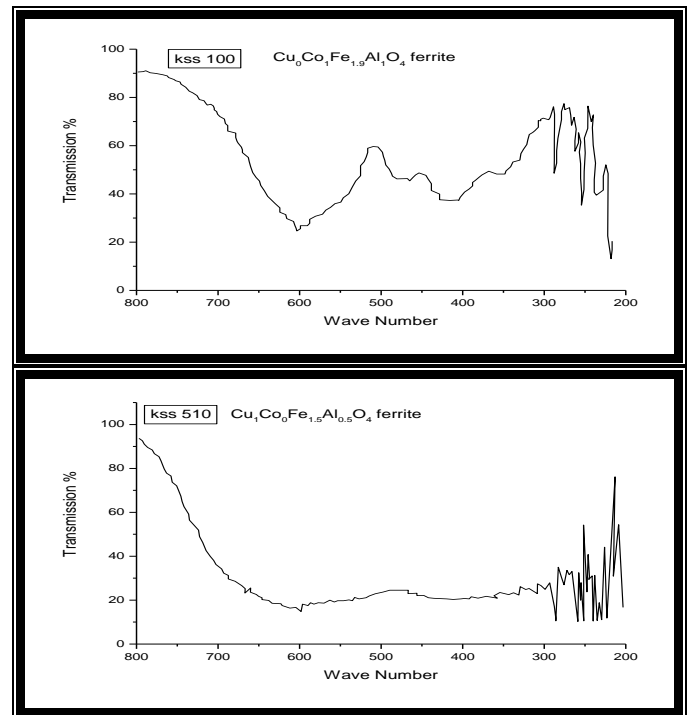


Figure 2: Absorption spectra for system $Cu_xCo_{1-x}Fe_{2-2y}Al_{2y}O_4$

The close inspection of all micrographs revealed that there is continuous grain growth with well – defined grain boundaries formed. The present system shows multi domain behavior. No exaggerated grain growth is observed in any composition. The average grain size is found to decrease with increase in Al content in copper cobalt ferrite. However in the present system the grain growth shows generally a decreasing trend with aluminum content, which is rather expected because of multi-domain behavior of these compositions in copper cobalt ferrite. Grain growth is almost accompanied with grain size, which is increasing with copper and aluminum content. So it appears that copper and aluminum content favors the grain growth. The scanning electron micrographs shown below

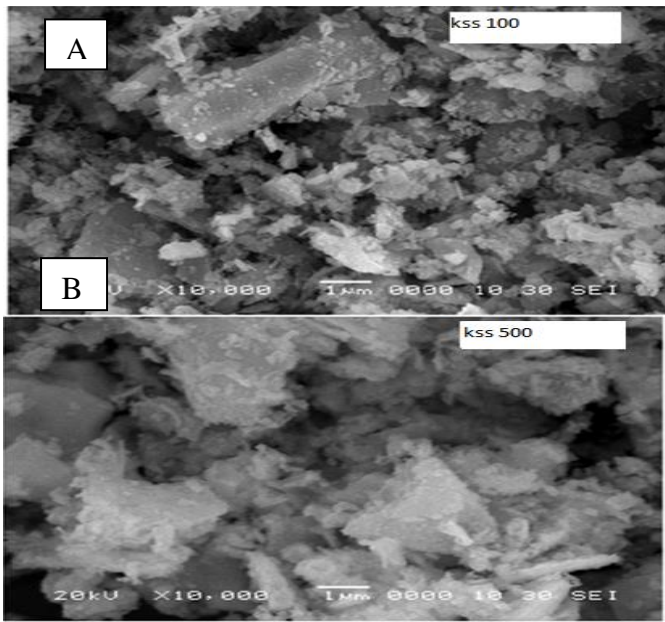


Fig: 3 (A) to (F) scanning electron microscopes of $Cu_xCo_{1-x}Fe_{2-2y}Al_{2y}O_4$:

(A) KSS 100- $Cu_0Co_1Fe_{1.9}Al_{0.1}O_4$,

(B) KSS 500- $Cu_0Co_1Fe_{1.5}Al_{0.5}O_4$

From the figures 4 it is found that Curie temperature of the compositions goes on decreases with increase in copper as well as aluminum content. It was rather expected because addition of copper replaces Fe^{3+} to B site reduces the population of Fe^{3+} on A site and hence A site becomes magnetically weak, results in the decrease in A-B interaction. Their Curie temperatures are determined by drawing tangent to the paramagnetic tail on the temperature axis. Similar type of paramagnetic tail and Curie temperatures determination has been reported [18, 19].

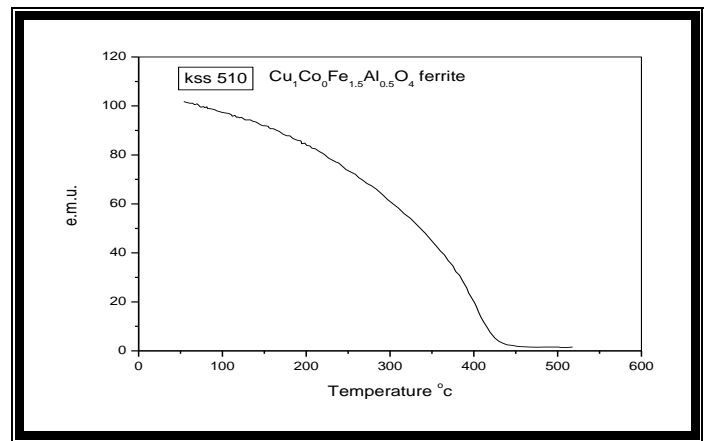
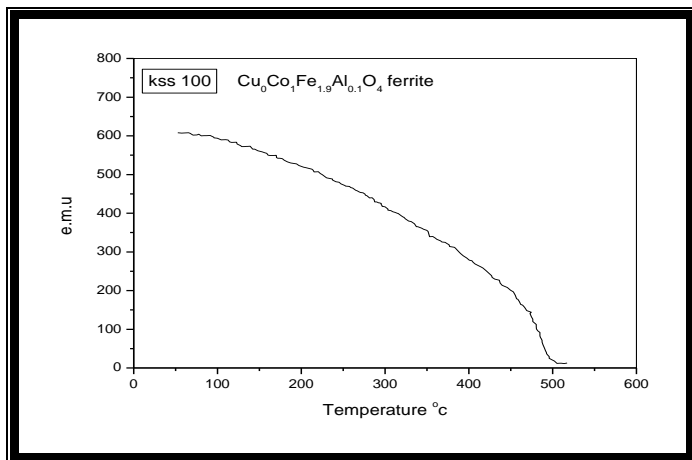


Fig 4: The curie temperatures for $Cu_xCo_{1-x}Fe_{2-2y}Al_{2y}O_4$ ferrite system

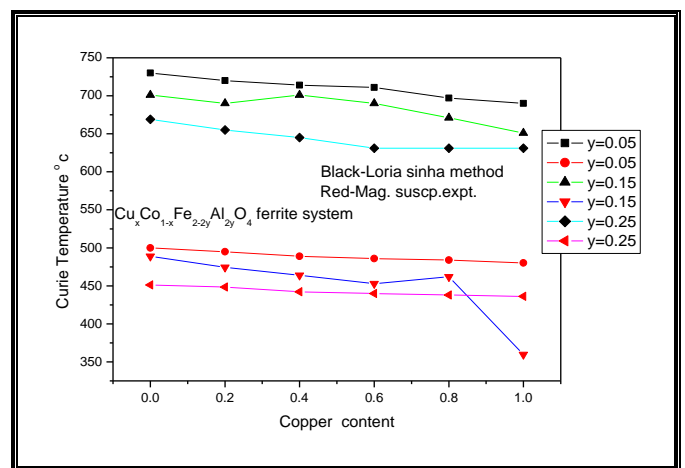


Fig4: Variation of curie temperature with copper and aluminum content for $Cu_xCo_{1-x}Fe_{2-2y}Al_{2y}O_4$ ferrite system

Curie temperature is the peculiar character of the ferromagnetic / ferrimagnetic materials. Curie temperature is the temperature at which it undergoes the phase transition from Ferro /Ferrimagnetic to paramagnetic state. The magnetic material shows spontaneous magnetization below its Curie point and no magnetization above the Curie temperature. In ferrites, Curie temperature is proportional to number of active magnetic linkages. It is affected by A-B distance and A-O-B angle. A-B interaction depends upon these distances. As these distance increases, Curie temperature decrease as suggested by Gorter and Neel [21-22] Curie temperature depends upon the Fe^{3+} ions participating in A-B interaction. When Fe^{3+} ions concentration per molecular formula unit is decreased, then Curie temperature decreased. Figure4

reveals the behaviour of Curie temperature in aluminium doped copper cobalt ferrite which is found decreasing with concentration of aluminium content indicating the decrease in ferrimagnetic properties.

IV. CONCLUSION

Copper cobalt ferrite is partially inverse spinel ferrite. Addition of Al^{3+} ions replaces Fe^{3+} on (B) site resulting in increase of lattice constant a , decrease in ionic radii (R_A) and bond length (O-A). The lattice constant obtained from XRD data shows increases. Curie temperatures of ferrite samples estimated by above mentioned three techniques are found in good agreement with each other. The curie temperature of copper cobalt ferrite decreases with aluminum and copper content.

V. REFERENCES

- [1]. R. S. Devan, S. A. Lokare, S. S. Chougule, D. R. Patil, Y. D. Kolekar, and B. K. Chougule, *J. Phys. Chem. Solids* 67, 1524 (2006).
- [2]. K. Zhao, K. Chen, Y. R. Dai, J. G. Wan, and J. S. Zhu, *Appl. Phys. Lett.* 87, 162901 (2005).
- [3]. S. R. Kulkarni, C. M. Kanamadi, and B. K. Chougule, *Mater. Res. Bull.* 40, 2064 (2005).
- [4]. Zhao L, Yang H, Yu L, Cui Y, Zhao X, Zou B, Feng SJ. *MagnMagn Mater* 2006;301:445–51.
- [5]. Rath C, Sahu KK, Anand S, Date SK, Mishra NC, Das RP. *J MagnMagn Mater* 1999;202:77–84.
- [6]. Rajendran M, Pullar RC, Bhattacharya AK, Das D, Chintalapudi SN, Majumdar CK. *J MagnMagn Mater* 2001;232:71–83.
- [7]. Ozaki M. *Mater Res Bull* 1989;12:35–43.
- [8]. Costa ACM, Tortella E, Morelli MR, Kaufman M, Kiminami RHGA. *J Mater Sci* 2002;37:3569–72.
- [9]. M.M. Mallapur, B.K. Chougule; *Materials Letters*; Vol. 64 (2010); P. 231–234.
- [10]. H. P. Klug, L. E. Alexander, *X-ray diffraction procedure for polycrystalline and amorphous materials*, Willey N.Y, 1997, 637.
- [11]. A. B. Gadkari, T. J. Shinde, P. N. Vasambekar, *J. Mater Sci: Mater Electron* 21 2010, 96 , 103.
- [12]. Prince E., Treuting R.G; *Acta Crystallographica*, 1956, 9, 1025.
- [13]. Sagal K., Tabellen F. *Rontegenstrukturanalyse*, Springer, Berlin, 1958.
- [14]. Borisenko A., Toropov N. A; *Z. Prikl Chem*, 1950, 23, 1165.
- [15]. Goodenough J.B and Loeb A. L ,*Phys. Rev.*, 1955, 98, 391.
- [16]. Waldron R.D, *Phy. Rev*, 1955, 99(6), 1727.
- [17]. K. V. S. Badarinath, *Phys. Stat. Solidi (a)* 1985, 91, 19-23.
- [18]. Karche B. R, Khasbardar B.V., and Vaingankar A. S., *J. Mag. and Mag. Mater.* 168 (1997) 292.
- [19]. Naik A.B., Sawant S.R., Patil S.A., and Pawar J.I., *Bull. Mater. Sci.*, 12 (3)(1989)1.